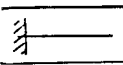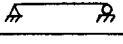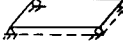Table 1 Resonant frequencies and damping coefficient by half-power method of the sandwich beam and plate with different boundary conditions

	ω_1 & ζ_1		ω_2 & ζ_2		ω_3 & ζ_3	
Peak Frequency	37	(40)*	222	(238)	611	(668)
Half-Power Frequency	35	38	198	240	507	664
Damping Coefficient	.041	(.039)	.095	(.092)	.128	(.095)

	ω_1 & ζ_1		ω_2 & ζ_2		ω_3 & ζ_3	
Peak Frequency	119	(113)	414	(425)	?	
Half-Power Frequency	112	126	?	451		
Damping Coefficient	.059	(.048)	.091**	(.091)		

	ω_{11} & ζ_{11}		ω_{21} & ζ_{21}		ω_{31} & ζ_{31}	
Peak Frequency	122	(126)	182	(196)	277	(309)
Half-Power Frequency	114	127	?	199	238	316
Damping Coefficient	.053	(.060)	.093**	(.073)	.141	(.091)

*Numbers in parenthesis are calculated data.
**This coefficient is based upon only the right half-power point by assuming symmetry.

Results and Discussion

The half-power method is used for this preliminary evaluation of Eq. (1) with an expected relatively high error in measured damping coefficients. The experimental procedure is standard. The harmonic excitation is varied through the frequency range of interest, the frequency response of the structure constructed, and then the peak frequency and corresponding half-power frequencies read. Details of this procedure can be found in Ref. 5. An aluminum beam, 9 in. long, 0.065 in. thick, covered with a 0.022-in. DuPont viscoelastic damping material and by an additional 0.020-in. aluminum constraining layer, subjected to simply supported and cantilever boundary conditions is considered. The measured and calculated results are shown in Table 1. In the simply supported beam case the lower half-power point of the second resonance could not be measured as is shown in Fig. 2. Data for a simply supported sandwich plate of 19.75 in. long by 9.75 in. wide with the same thickness configuration of the beam are also shown in this table.

The error between measured and calculated data with respect to the measured data for resonant frequencies is from 2% to 11% for all the resonances shown in Table 1. The experimental measurement of resonant frequencies itself is accurate within 1 Hz. Thus it is believed that Eq. (1) predicts the resonant frequencies for the sandwich beam as accurate as the classical beam equation for an uniform elastic beam.

The error between measured and calculated data with respect to the measured data in damping coefficients is from 0% to 35%. This error arises from many possible sources; however, the mingling of the resonance tails is the prevailing source in most cases. Although this damping error is relatively high, it is believed that a well-designed high damping measurement method for the constrained-layer damping could reduce the error.

Additional discussion and comparison of calculated data using the present theory with the experimental data obtained by the decay method on various sandwich configurations reported in NASA CR-742 (Ref. 6) are also given in Ref. 5. These tend to strengthen the aforementioned conclusions.

References

[1] Ross, D., Ungar, E. E., and Kerwin, E. M., Jr., "Damping of Plate Flexural Vibrations by Means of Viscoelastic Laminae," Colloquium on Structural Damping, ASME, New York, Dec. 1959, Sec. 3, pp. 50–87.

[2] DiTaranto, R. A., "Theory of Vibratory Bending for Elastic and Viscoelastic Layered Finite-Length Beams," Transactions of the ASME, Journal of Applied Mechanics, 1965, pp. 881–886.

[3] Mead, D. J. and Markus, S., "The Forced Vibration of a Three-Layer, Damped Sandwich Beam with Arbitrary Boundary Conditions," Journal Sound Vibration, Vol. 10, No. 2, 1969, pp. 163–175.

[4] Yan, M.-J. and Dowell, E. H., "Governing Equation for Vibrating Constrained-Layered Damping in Sandwich Plates and Beams," Transactions of the ASME, Journal of Applied Mechanics, Nov. 1972, to be published.

[5] Yan, M.-J., "Constrained-Layer Damping in Sandwich Beams and Plates," Ph.D. thesis, June 1972, Princeton Univ.; also AMS Rept. 1031, June 1972, Princeton Univ., Princeton, N.J.

[6] Ruzicka, J. E., Derby, T. F., Schubert, D. W., and Pepi, J. S., "Damping of Structural Composite with Viscoelastic Shear-Damping Mechanics," NASA CR-742, March 1967.

Engineering Analysis of Reattaching Shear Layer Heat Transfer

D. E. NESTLER*
General Electric Company, Philadelphia, Pa.

Nomenclature

H = total enthalpy
$I_2(\eta_j)$ = Korst-Chow integral (Ref. 5)
M = Mach number
n = exponent in wall jet heat flux decay [Eq. (4)]
p = static pressure
Pr = Prandtl number
$\dot{q}$ = wall heat flux
Re = Reynolds number
St = Stanton number
T = temperature
U = velocity
X_R = recirculation distance from location of maximum heat flux (Fig. 1)
β = flow reattachment angle (Fig. 1)
Δ_D = shear layer width above dividing streamline (Fig. 1)
λ = freestream turbulence heating augmentation factor
μ = absolute viscosity
ρ = density
σ = turbulent shear layer spread parameter

Subscripts

D = dividing streamline
e = edge of boundary layer or shear layer
max = maximum
s = stagnation
w = wall
o = at compression ramp corner

1 = immediately upstream of separation
2 = downstream of separation; also, behind normal shock
3 = downstream of reattachment

Superscripts

ε = exponent index; $\varepsilon = 0$ for laminar shear layers; $\varepsilon = 1$ for turbulent shear layers

AN engineering analysis is developed which yields reasonable predictions of maximum reattachment heat transfer for laminar or turbulent separated shear layers, as well as heat flux distribution in the regions upstream and downstream of reattachment. The analysis is based on an analogy to jet impingement heat transfer in the reattachment region, a wall jet heating decay in the recirculation region, and a new boundary layer downstream of reattachment whose growth is controlled by local reattaching shear layer flow properties. Upstream boundary-layer thickness effects are included by use of appropriate pre-asymptotic shear layer profiles. In general, better agreement of prediction with experiment is obtained for laminar separation/reattachment. Maximum reattachment heating for turbulent separation was found to exceed prediction of the jet impingement model by significant amounts, probably because of large scale flow unsteadiness and reattachment pressure fluctuations. A simple empirical expression based on reattachment pressure ratio was found to yield satisfactory predictions for the turbulent case.

A conceptual model of separated/reattaching flow is shown in Fig. 1. This class of reattaching flow is termed "full shear layer reattachment," since the entire shear layer reattaches to the deflecting surface. The expression for maximum reattachment heat flux is based on the two-dimensional form of the Lees laminar stagnation point heat flux relation, with a velocity gradient $(dU/dS)_o = U_2/\Delta_D$, in analogy with two-dimensional jet impingement. The effect of incidence is approximated by assuming $\dot{q}_s \sim P_s^{0.5}$, with the hypersonic approximation $p_s \sim (M \sin \beta)^2$. The resulting relation is

$$\dot{q}_s = 0.50\lambda^\varepsilon(\rho_e U_e \mu_s/\Delta_D)^{0.5}(H_s - H_w)\sin\beta/Pr^{2/3} \qquad (1)$$

in which the factor λ attempts to allow for local freestream turbulence effects, as defined by Nestler.[1] Alternate expressions for maximum reattachment heat flux for turbulent shear layers are also considered.

a) Turbulent shear layer energy exchange, as suggested by Donaldson[2]

$$\dot{q}_{max} = \rho_D U_D(H_D - H_w)I_2(\eta_j)/\sigma \qquad (2)$$

b) Empirical method, as employed, e.g., by Kim and Parkinson[3]

$$\dot{q}/\dot{q}_1 = (p/p_1)^{0.8} \qquad (3)$$

In Eq. (3), the local reattachment pressure p is computed as the stagnation pressure behind a normal shock corresponding to p_2 and M_{2_N}, the component of M_2 normal to the reattachment surface.

Another class of reattaching flow is that of "partial shear layer reattachment," such as that of flow over a surface cavity, in which only the lower portion of the shear layer reattaches to the deflecting surfaces. In Ref. 1, a relation similar to Eq. (1) is derived for partial shear layer reattachment, using dividing
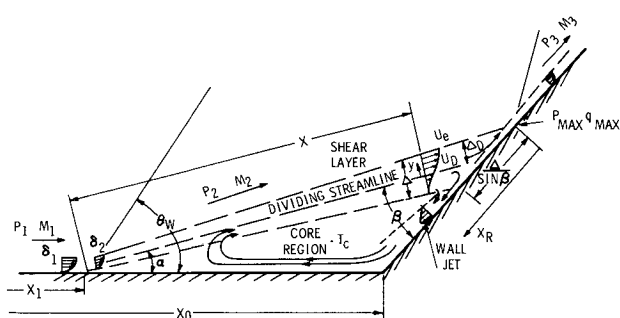

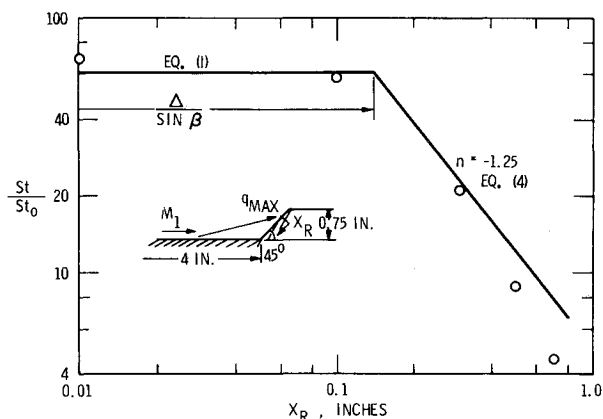Fig. 1   Full shear layer reattachment flow model.

Fig. 2   Reattachment heat flux distribution on 45° compression step in hypersonic laminar flow (data of Holden, $M_1 = 10$, $Re/\text{in.} = 1.35 \times 10^5$, $T_w/T_s = 0.23$).

streamline properties rather than shear layer edge properties, and an empirically determined effective shear layer width.

Shear layer profiles are evaluated by techniques which include the effect of upstream boundary-layer thickness. For laminar shear layers, the similarity solutions of King and Baum[4] are used. For turbulent shear layers, the asymptotic dividing streamline velocity ratios of Korst and Chow[5] are modified by the method of Alber and Lees.[6]

Heat flux distribution in the recirculation region is assumed to correspond to a wall jet heat flux decay†

$$\dot{q} \sim X_R^n \qquad (4)$$

in which X_R is measured from the location of maximum reattachment heat flux. In Eq. (4), $n = -1.25$ for laminar flow (Glauert[7]) and $n = -0.6$ for turbulent flow (Akfirat[8]).

Heat flux distribution downstream of reattachment is modeled as a boundary layer having its origin at reattachment, whose development is determined by local external flow properties. Assuming flat plate heating relations for simplicity, the following relation results

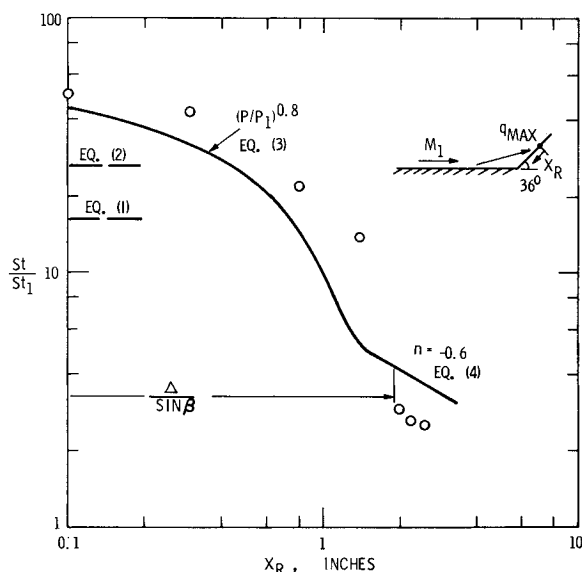$$\dot{q}_3/\dot{q}_1 = (\rho_3 U_3/\rho_1 U_1)^a(\mu_3 X_1/\mu_1 X_3)^b \qquad (5)$$

Fig. 3   Reattachment heat flux distribution on 36° compression ramp in hypersonic turbulent flow (data of Holden, $M_1 = 11.3$, $Re_{x1} = 35 \times 10^6$, $T_w/T_s = 0.19$).

† This approximation will be in error because of streamwise pressure gradient effects in the region of formation, as well as mass addition effects from the reattaching shear layer.

in which $a = b = 0.5$ for laminar flow and $a = 0.8$, $b = 0.2$ for turbulent flow. In Eq. (5), the properties $\rho_3 U_3$, and μ_3 correspond to the inviscid edge values in the case of full shear layer reattachment, and to limiting streamline properties in the case of partial shear layer reattachment.

Comparisons of the predictions of the analysis with a sampling of previously published heat transfer measurements obtained on a variety of reattachment geometries are given in Ref. 1, including cavities, compression ramps, spike nosed body, and forward facing step. Representative comparisons are shown in Figs. 2 and 3 for laminar and turbulent separation/reattachment over compression ramps. In Fig. 2, the maximum laminar reattachment heating level measured by Holden[9] is well predicted, as is the decay in the recirculation region. In Fig. 3, Eqs. (1) and (2) are seen to seriously underpredict the maximum turbulent reattachment heating level measured by Holden.[10] However, the simple empirical relation of Eq. (3) yields reasonable agreement with the data.

The method presented herein offers a generalized approach for predicting both laminar and turbulent shear layer reattachment heating. Previously published methods are confined to semi-empirical correlations applicable for specific geometries and type of flow.

References

[1] Nestler, D. E., "An Engineering Analysis of Reattaching Shear Layer Heat Transfer," AIAA Paper 72-717, Boston, Mass., 1972.

[2] Donaldson, C. duP., private communication, Feb. 1969,

[3] Kim, B. S. C. and Parkinson, T. W., "Flap Turbulent Heating Characteristics Obtained from a Hypersonic Shock Tunnel," *Journal of Spacecraft and Rockets*, Vol. 9, No. 4, April 1972, pp. 227–228.

[4] King, H. H. and Baum, E., "Enthalpy and Atom Profiles in the Laminar Separated Shear Layer," RN-8, March 1963, Electro-Optical Systems Inc., Pasadena, Calif.

[5] Korst, H. H. and Chow, W. L., "Non-Isoenergetic Turbulent $(Pr_t = 1)$ Jet Mixing Between Two Compressible Streams at Constant Pressure," NASA CR-419, April 1966.

[6] Alber, I. E. and Lees, L., "Integral Theory for Supersonic Turbulent Base Flows," *AIAA Journal*, Vol. 6, No. 7, July 1968, pp. 1343–1351.

[7] Glauert, M. B., "The Wall Jet," *Journal of Fluid Mechanics*, Vol. 1, 1956, pp. 625–643.

[8] Akfirat, J. C., "Transfer of Heat from an Isothermal Flat Plate to a Two-Dimensional Wall Jet," *Proceedings of the 3rd International Heat Transfer Conference*, AIChE, New York. Vol. 2, 1966, pp. 274–279.

[9] Holden, M. S., "Experimental Studies of Separated Flows at Hypersonic Speeds. Part 2: Two-Dimensional Wedge Separated Flow Studies," *AIAA Journal*, Vol. 4, No. 5, May 1966, pp. 790–799.

[10] Holden, M. S., "Shock Wave—Turbulent Boundary Layer Interaction in Hypersonic Flow," AIAA Paper 72-74, San Diego, Calif., 1972.

Self-Weight-Buckling of Vertical Circular Cylindrical Shells

D. J. JOHNS*

University of Technology, Loughborough, Leicestershire, England

Nomenclature

a = shell radius
c = radial deflection amplitude
D = shell rigidity $Eh^3/12(1-v^2)$
E = Young's modulus
h = shell thickness
l = shell length
m = number of axial waves or half-waves

n = number of circumferential waves
r = parameter in Sec. 3
w = radial deflection
x = axial coordinate
σ = axial stress
θ = circumferential coordinate
v = Poisson's ratio

1. Introduction

IN Ref. 1 experimental results for rubber cylinders were given for the title subject and a comparison was made with the existing classical theoretical result for such shells subjected to a uniform axial compressive stress. It was assumed intuitively that such a result would apply when the axisymmetric axial compressive stress varied linearly (due to self-weight). In fact, the agreement was very good for thicker (taller) shells, but became progressively less so for thinner (shorter) shells.

It should be noted that in Ref. 2 linear buckling analyses for asymmetric axial compressive stress distributions produced the result that the classical result was applicable to the asymmetric cases.

The purpose of the present Note is to attempt to show from a similar reasoning that the same classical result applies to self-weight buckling.

2. Review of Classical Results

Reference 3 presents the well-known result for the buckling of a rubber cylindrical shell under uniform axial compression, viz,

$$\sigma_1 = Eh/a[3(1-v^2)]^{1/2} \approx 0.667 Eh/a \quad (v = 0.5) \qquad (1)$$

This result is based on the assumption of a sinusoidal wave form axially and applies to symmetrical buckling ($n = 0$) or asymmetrical buckling ($n > 0$) provided that the cylinder is not too short and that a large number of axial waves is involved, i.e.,

$$m\pi a/1 \gg 1$$

For very long shells and when only a small number of axial waves is involved, the critical uniform axial stress is[3] equal to 0.6 x that of Eq. (1) and corresponds to a circumferential buckling mode in which $n = 2$—i.e. circular shell buckles into an ellipse. Thus,

$$\sigma_2 \approx 0.4 Eh/a \qquad (2)$$

Other analyses presented in Ref. 3 for inextensional buckling and for elemental strips of the shell buckling as "equivalent struts" of length 1 are not considered relevant in this case.

3. Present Analyses

A general analysis is presented in Ref. 3 for asymmetric buckling involving 3 coupled differential equations in the displacements in the axial, circumferential, and radial directions. For the problem of self-weight buckling with $\sigma = \sigma_o(1 - x/1)$ and with $w = c \sin n\theta \sin (m\pi x/2L)$ corresponding to an open-ended shell at $x = 1$, with m an integer, it is found that

$$\sigma_3 = 2\sigma_1 \quad \text{for} \quad m \geq 2 \qquad (3)$$

This result is believed to be too high.

For symmetrical buckling with $w = c[1 - \cos (2m\pi x/1)]$ $0 < x < 1/m$, corresponding to a single buckle at the base of the shell, and with self-weight loading, one finds from an energy analysis that

$$\sigma_4 = 1.732\sigma_1 \qquad (4)$$

Thus for a clamped base and with buckling initiating there, the critical stress is $(3)^{1/2}$x that for simple supports. However, it is possible that the preceding single assumed mode is not sufficiently realistic, and that with a greater number of assumed modes in the energy analysis a lower factor than $(3)^{1/2}$ would be obtained.

For symmetrical buckling with $w = c \cos^2(r\pi x/21) \sin (m\pi x/1)$ $0 < x < 1/r$ corresponding to a sinusoidal wave form which decreases in amplitude from $x = 0$ to zero at $x = 1/r$, one obtains the following general result: